Imperial College London

Cluster geometry and survival probability in systems driven by reaction-diffusion dynamics.

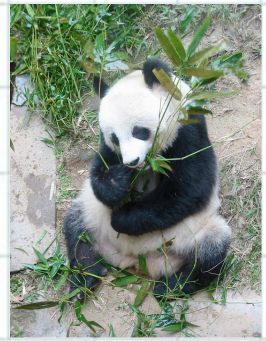

Henrik Jeldtoft Jensen
Institute for Mathematical Sciences
&
Department of Mathematics

together with
Alastair Windus

- now **The Home Office.**

Content

Motivation - Survival of populations

The model

- sexual reproducers
- mixture sexual-asexual

Sexual reproduction

- the Critical Behaviour

Ecology: Conservational implications – Allee effect

Geometry: - between 1 and 2 dimensions

Mixture of sexual asexual reproduction rates:

- continuous transition
- tricitical point
- 1^{st} order critical points
- cluster approximation
- geometrical structure of clusters

Motivation

Extinction of species happens at an ever increasing rate.

Causes:

- ☐ some of specific biological nature
- ☑ some due to fluctuations: small numbers
- ☑ sexual reproduction: partners have to be able to meet

statistical mechanics applied to conservation ecology

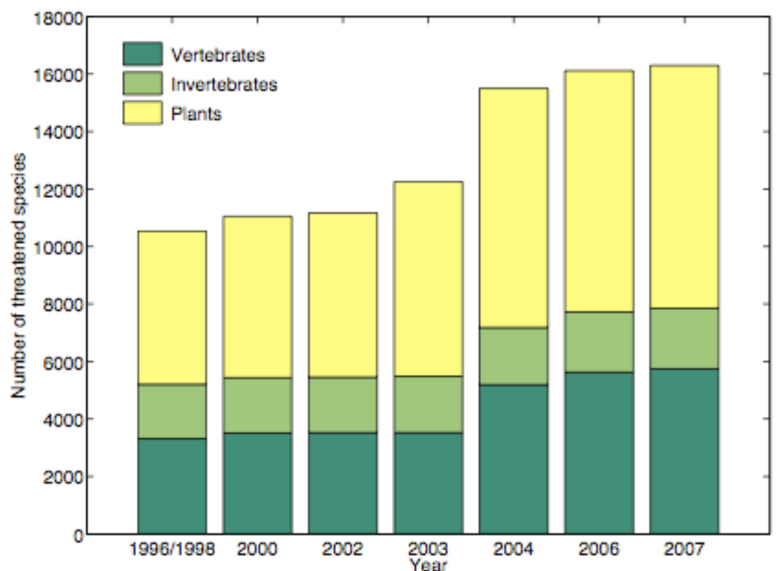

From http://www.iucnredlist.org/info/2007RL Stats Table%202.pdf.

What is the optimal size for a refuge?

Model

Die with probability: p_d

Sexual reproducing individuals

Move about by random walk

May reproduce when nearest neighbours: p_b

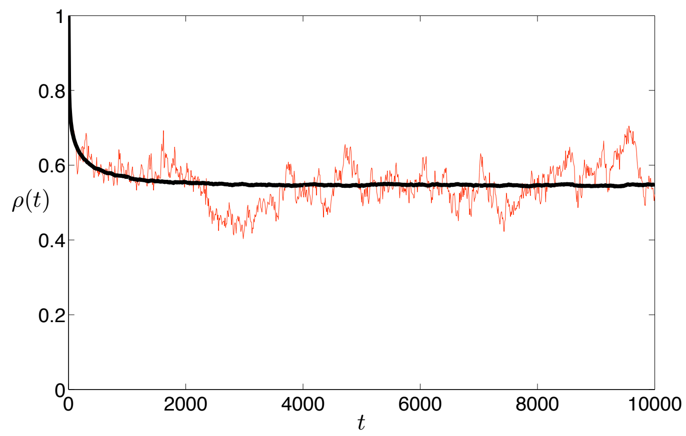

Figure 3.1: Two example plots in the (1+1)-dimensional simulations results with $p_b = 0.5$ and $p_d = 0.07$. The black plot is an average over 1,000 runs, whereas the red plot is the data from just one run.

Model Details

1) A set number of individuals are randomly placed on the lattice (usually we begin with all sites occupied).

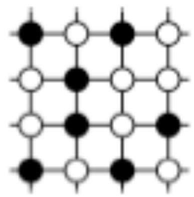

2) A site is chosen at random.

3) If the chosen site is empty, nothing happens. Return to 2).

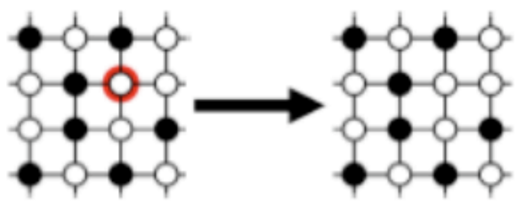

4) If the chosen site is occupied, the individual dies with probability p_d. If the individual dies, return to 2). Otherwise, continue to 5).

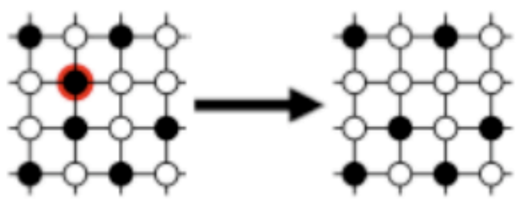

Henrik Jeldtoft Jensen
Imperial College London

Model Details

5) If the individual does not die, a neighbouring site is chosen at random. If this site is empty, the individual moves there and we return to 2). If the site is however occupied, continue to 6).

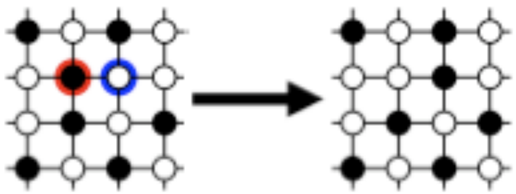

6) Another neighbouring site is chosen at random. If this site is occupied, nothing happens and we return to 2). Otherwise, a new individual is placed on this site with probability p_b.

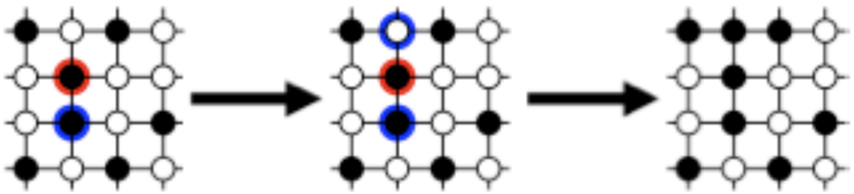

Mean field equation

$$\frac{d\rho(t)}{dt} = p_b(1-p_d)\rho^2(t)[1-\rho(t)] - p_d\rho(t)$$

$$\bar{\rho}_0 = 0 \text{ or } \bar{\rho}_\pm = \frac{1}{2}[1 \pm \sqrt{1 - \frac{4p_d}{p_b(1-p_d)}}]$$

For $\rho(0) = 1$

$$\lim_{t\to\infty} \bar{\rho}(t) = \bar{\rho}_+ \text{ for } p_d \leq p_{d_c}$$

$$p_{d_c} = p_b/(4+p_b)$$

The spatio-temporal process

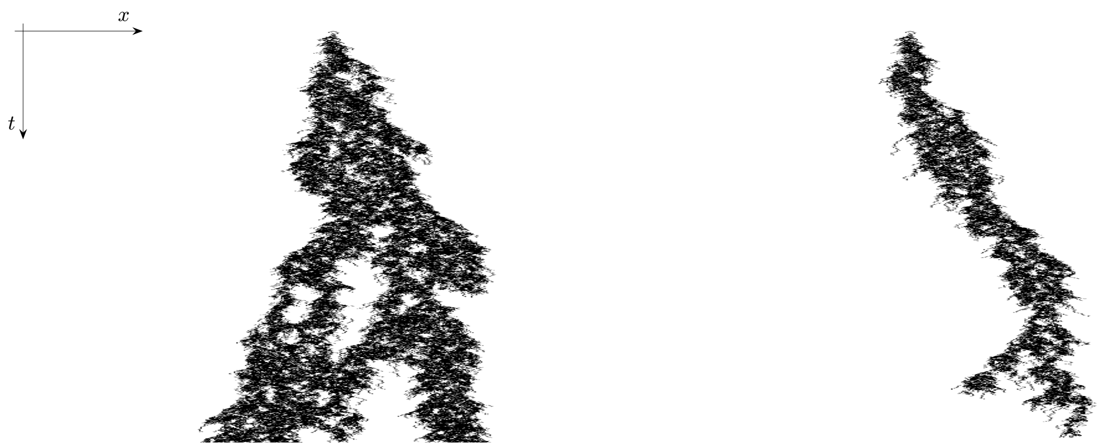

Figure 3.4: Space-time plots showing examples where the population survives (left) and dies out (right) for $t_{\mathrm{max}} = 2,000$. A value of $p_{\mathrm{b}} = 0.5$ was used in both cases with $p_{\mathrm{d}} = 0.071$ in the left plot and $p_{\mathrm{d}} = 0.075$ in the right.

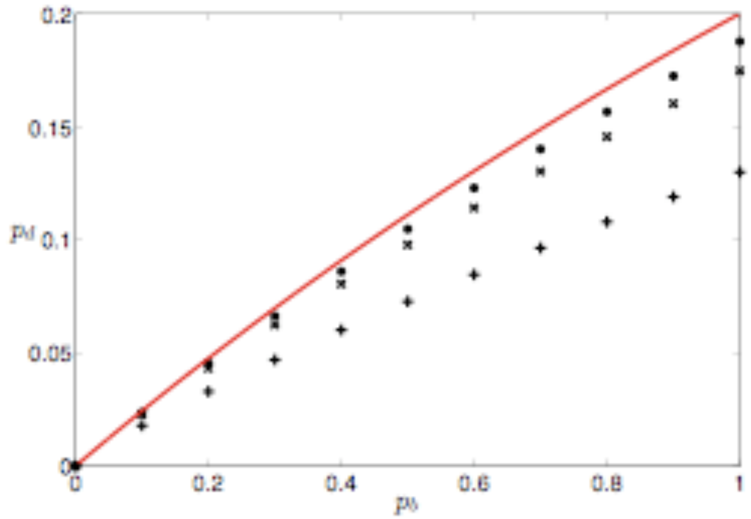

Figure 3.3: Critical parameter values for the MF (line), $1+1$ ($+$), $2+1$ ($\times$) and $3+1$ ($\bullet$) dimensional simulations.

Density dependence of survival probability known as Allee effect.

Below $\bar{\rho}_-$ extinction

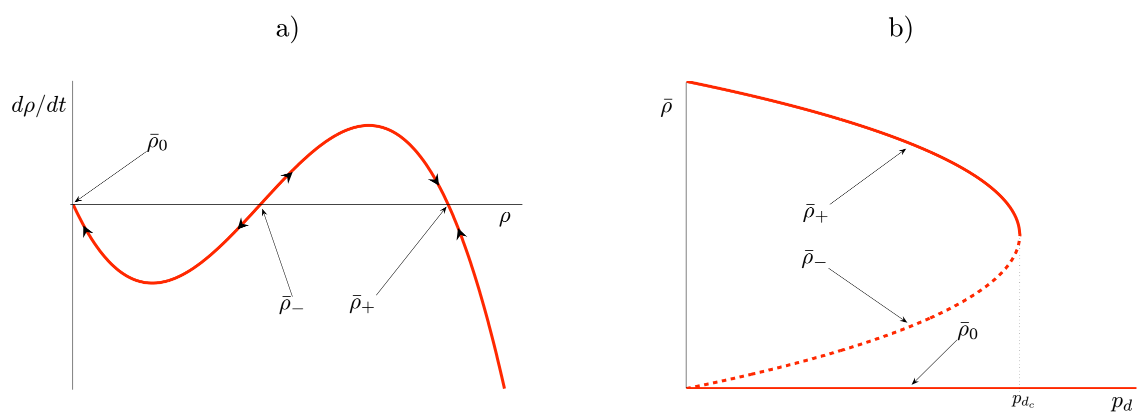

Figure 3.5: a) $d\rho/dt$ versus ρ showing the (in)stability of the stationary points $\bar{\rho}_+$, ($\bar{\rho}_-$) and $\bar{\rho}_0$. b) Bifurcation diagram according to the MF equation where solid lines show the stable, and hashed lines the unstable, steady states.

Extinction as phase transition

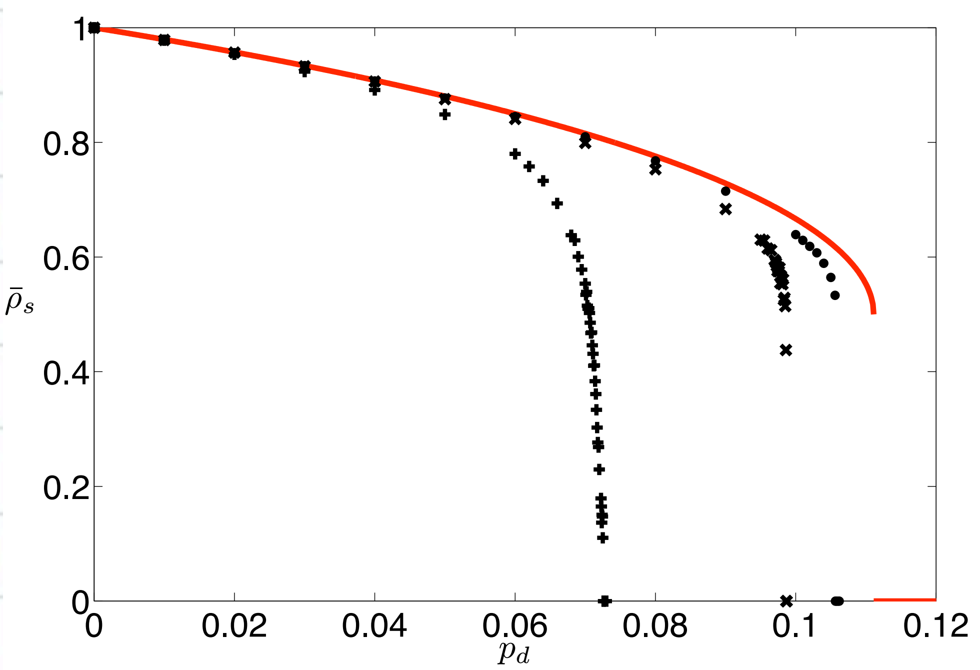

Extinction as a phase transition

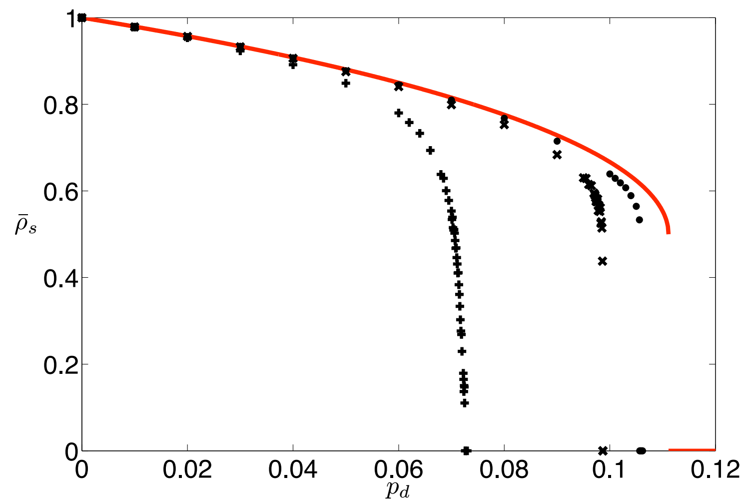

Figure 4.1: Steady state population densities for the MF (line) and the $(1+1)$- $(+)$, $(2+1)$- $(\times)$ and $(3+1)$- $(\bullet)$ dimensional MC simulations.

Discontinuous change for d> 1

Continuous change for d = 1 → look for $\rho(t) \propto t^{-\delta}$

A. Windus and H.J. Jensen,
Phase transitions in a lattice population model.
J Phys A, 40, 2287-2297 (2007).

d=1:
Exponents consistent with
Directed Percolation class

Continuous transition: Algebraic indicator

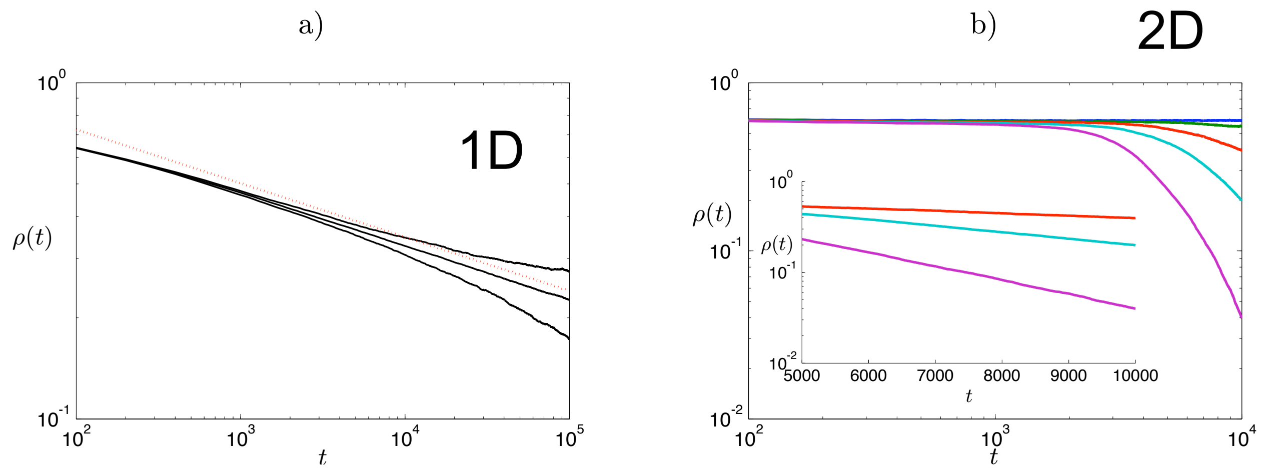

Figure 4.2: a) Log-log plots showing power law behaviour at the critical point for the (1+1)-dimensional model (middle black line) and non-power law behaviour for the off critical points. The black lines represent (from top to bottom) $p_{\mathrm{d}} = 0.071654$, 0.071754 and 0.071854. The red line represents the gradient -0.159 as a guide for the eye. b) Non-power law behaviour for various values of p_{d} close to the critical point for the $2+1$ dimensional model. The exponential decay for the super-critical values are shown in the inset. The $3+1$ dimensional case is very similar. Information on how the critical points were found are detailed later in this chapter.

Discontinuous transition: hysteresis

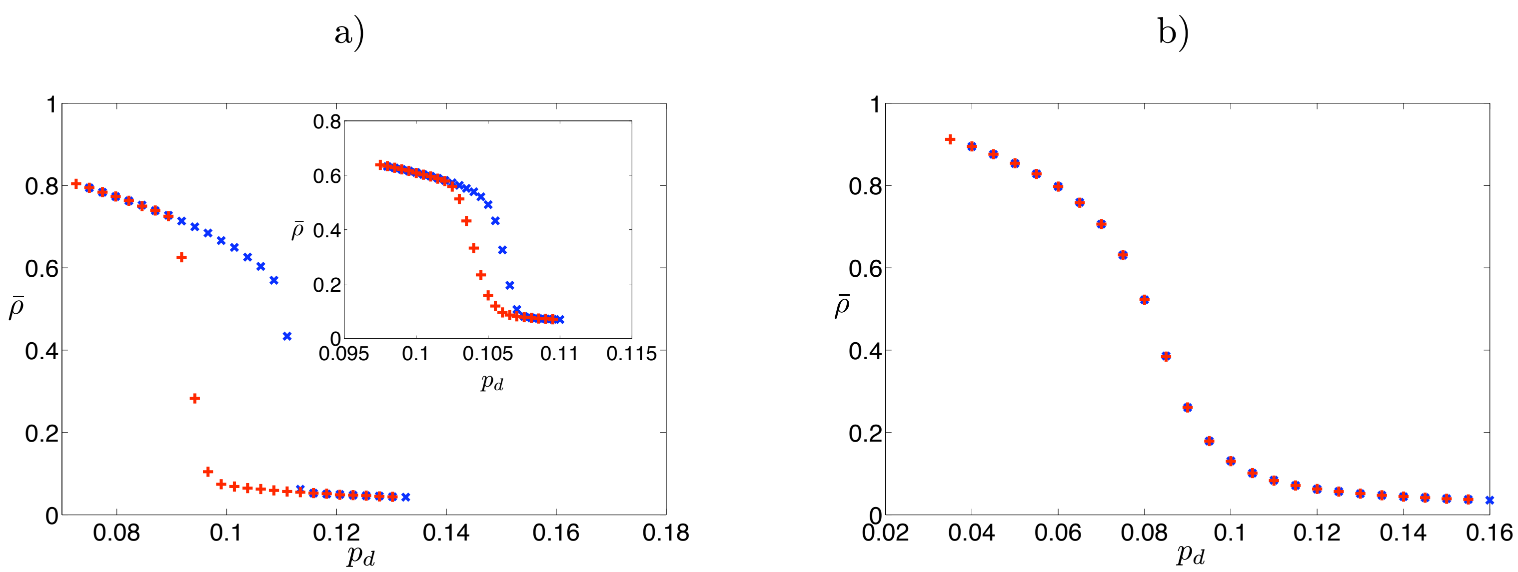

Figure 4.3: Hysteresis loop for the a) (2+1)- (inset) and (3+1)-dimensional models and b) no hysteresis occurring in the (1+1)-dimensional model. The ticks show p_d increasing ($\times$) and decreasing ($+$).

Continuous transition in d = 1

At $p_d = p_{d_c}$ expect survival prob

and population size to scale as

$$P(t) \sim t^{-\tau}$$
$$n(t) \sim t^{\eta}$$

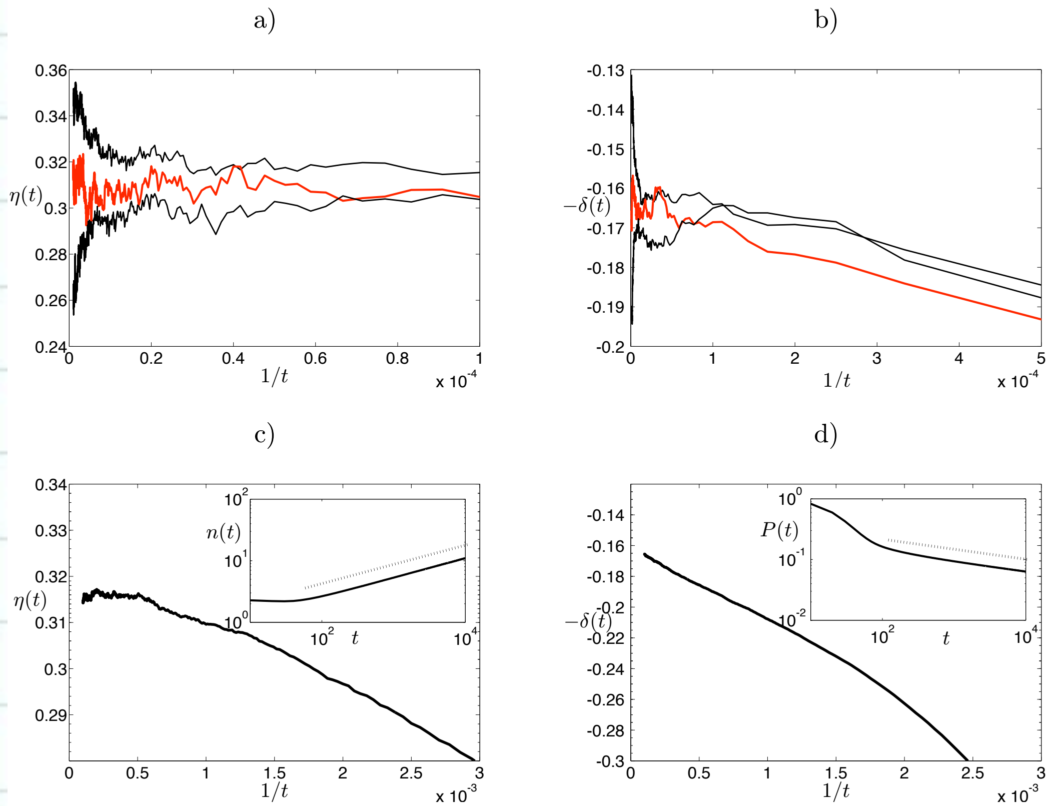

Figure 4.4: Plots of a) $\eta(t)$ and b) $\delta(t)$ up to $t = 10^6$. From top to bottom, $p_{\mathrm{d}} =$ 0.071746, 0.071754 (red) and 0.071762. Plots c) and d) show the same but only up to $t = 10^4$ and with $p_{\mathrm{d}} = p_{\mathrm{d_c}} = 0.071754$ only. The insets show the plots of $n(t)$ and $P(t)$ with the hashed lines showing the gradients of η and δ respectively.

Asymptotic values

$$\eta = 0.314 \pm 0.002$$
$$\delta = 0.160 \pm 0.00.2$$

consistent
with Directed Percolation
universality class

$$\eta = 0.313686$$
$$\delta = 0.159464$$

First order in d $\geqq$ 2

Histogram indicators

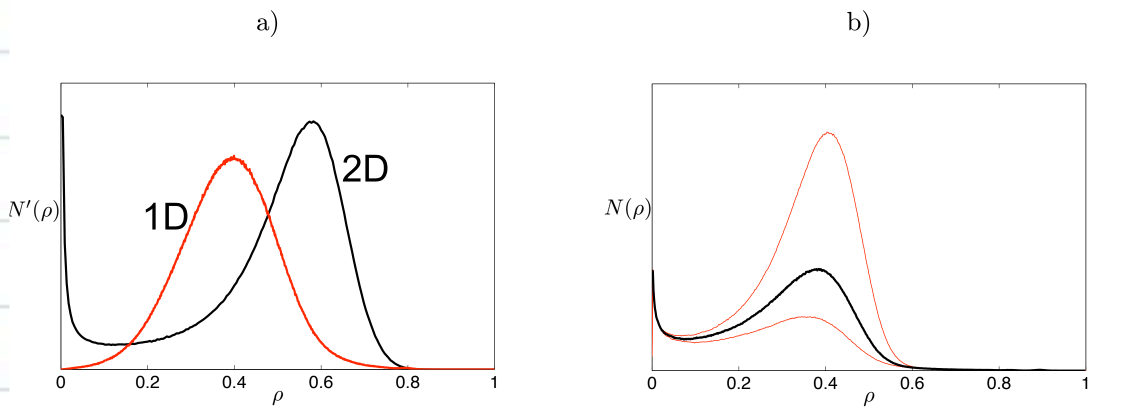

Figure 4.8: a) Normalised histogram, $N'(\rho)$ for different population densities in the $(1+1)$-dimensional (left) and $(2+1)$-dimensional (right) cases showing the results at the critical point for a continuous and first-order phase transition respectively. b) Example of output at the critical point $p_{\mathrm{d_c}}$ with $p_{\mathrm{d_c}} - 0.001$ (top) and $p_{\mathrm{d_c}} + 0.001$ (bottom) in the (2+1)-dimensional case.

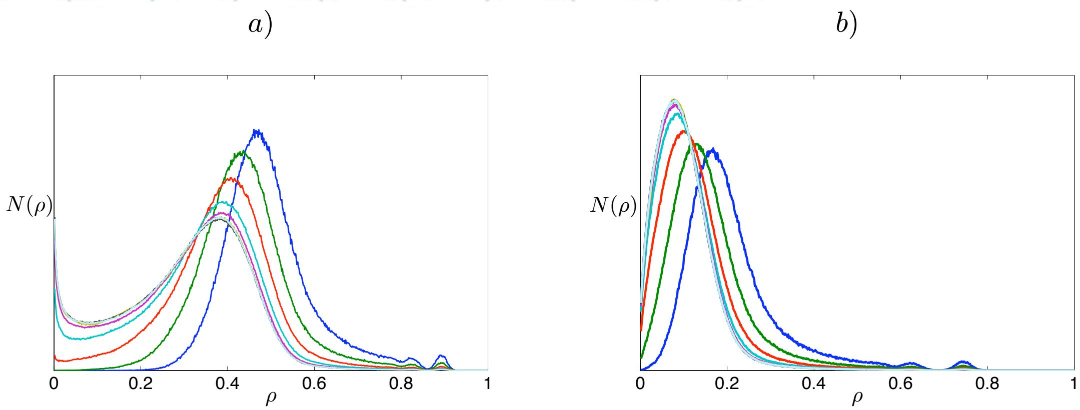

Figure 4.9: Histogram of population density for different number of time steps at a) a first-order phase transition and b) a continuous phase transition. In both cases, from right to left, t = 100, 200, 400, 800, 1600, 3200, 6400 and 12800.

Size dependence

The value of p_{d_c} in the limit $L \to \infty$

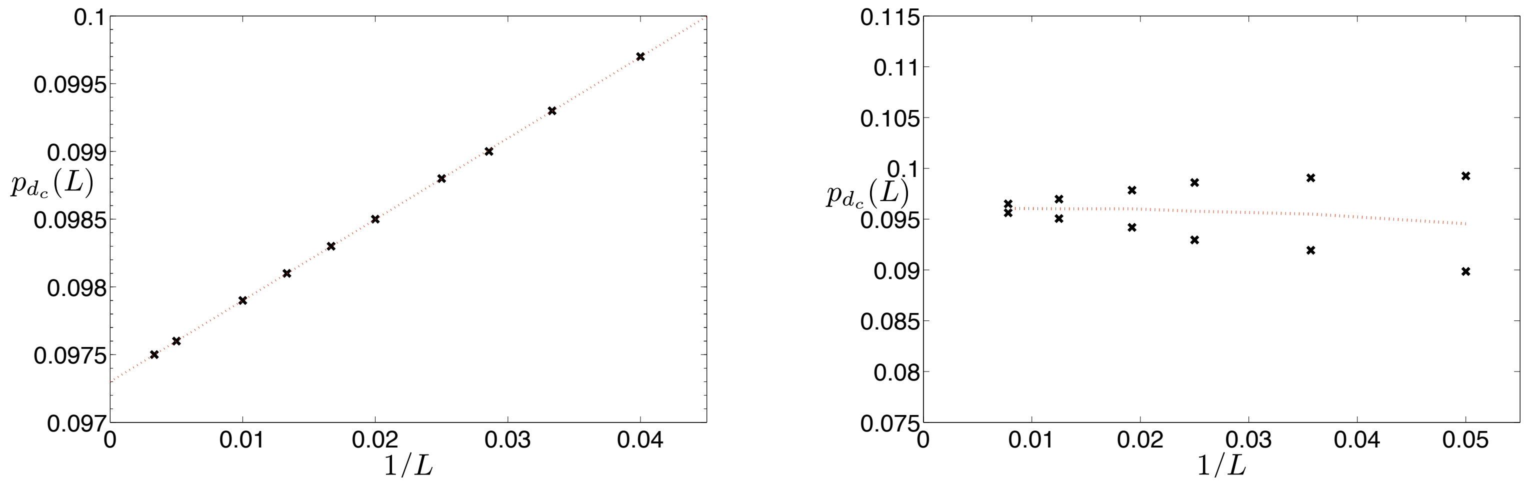

Figure 4.10: L-dependent critical point in 2+1 dimensions for a) our histogram method and b) the interface method. In a) the red hashed line shows the line of best fit, extrapolating to the thermodynamic limit and in b), it shows the mean value of p_{d_1} (top) and p_{d_2} (bottom).

Interface Method

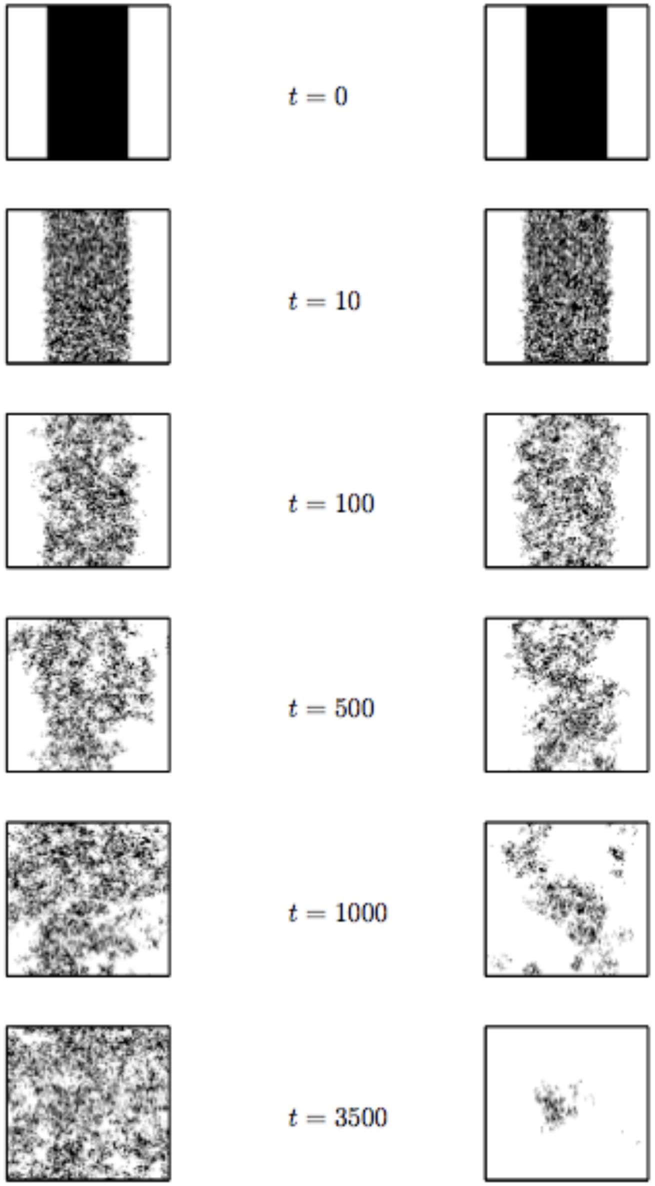

Figure 4.11: Snapshots showing the dynamics of the population at different time steps for $p_d < p_{d_c}$ (left) and $p_d > p_{d_c}$ (right).

Between one and two dimensions

http://www.fractalism.com/fractals/dragon.htm

Does the change in the nature of transition occur for d between 1 and 2 dimensions?

Fractals of different fractal mass dimensions

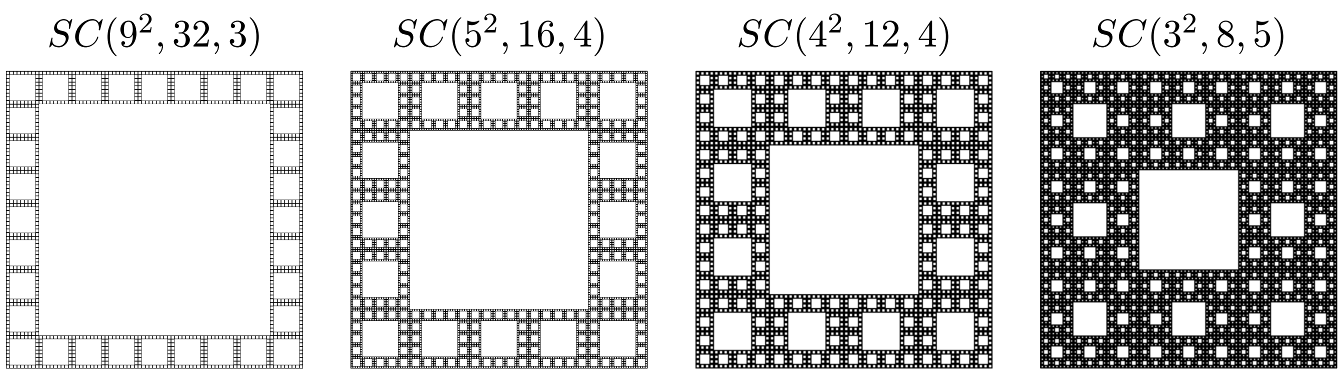

Figure 4.12: Pictures of Sierpinski carpets of various fractal dimensions. Although a finite value of κ was used in each case, we give the approximate fractal dimensions as (from left to right) $d_f \simeq \log(32)/\log(9) = 1.5573$, $\log(16)/\log(5) = 1.7227$, $\log(12)/\log(4) = 1.7925$ and $\log(8)/\log(3) = 1.8928$ (all to 4 decimal places).

A. Windus and H.J. Jensen,
Change in order of phase transition on fractal lattice.
Physica A **388**, 3107 (2009)

Change in nature of transition appears to happen for d ≃ 1.7

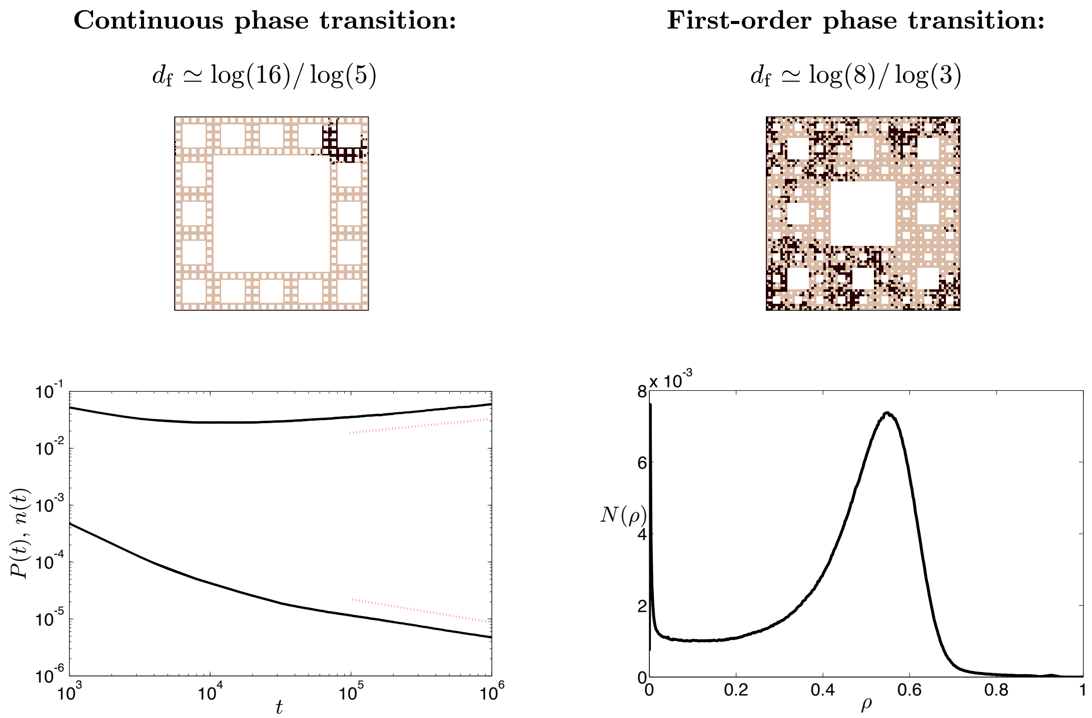

Figure 4.13: Results and snapshots of the simulations for the continuous (left) and first-order (right) phase transitions. For the continuous phase transition, we have used a single seed and we see the resulting power law behaviour along the hashed lines. For the first-order phase transition we began the simulations from a fully-occupied lattice and we observe the double-peaked structure in the histogram of population density.

Scaling relation for $d_f < d_c$

$$\eta + 2\delta = d/z \rightarrow \eta + 2\delta = d_f/z$$

Measure η and δ in simulations from

$$P(t) \quad \bar{\propto} \quad t^{-\delta}$$
$$n(t) \quad \bar{\propto} \quad t^{\eta}$$

and estimate z from $$z_{scaling} = \frac{d_f}{\eta + 2\delta}$$

compare with the directly measured value of z from

$$R^2(t) \bar{\propto} t^{2/z}$$

Behaviour below and above d=1.7

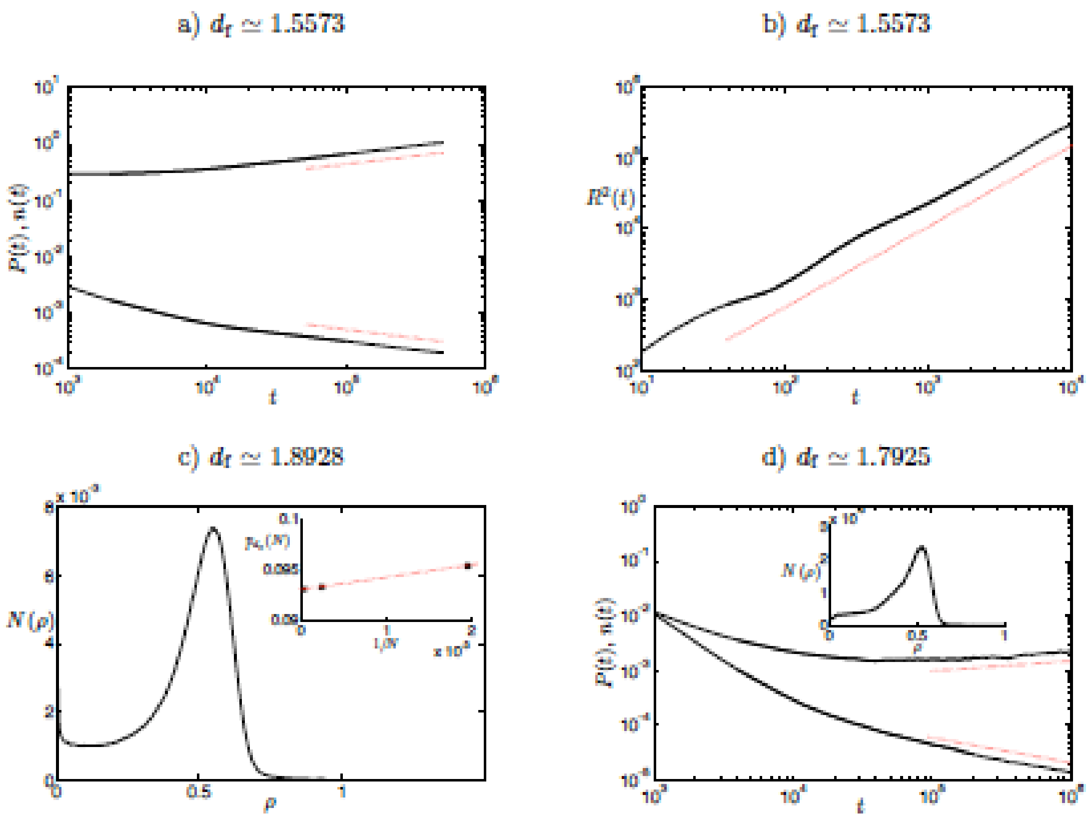

Figure 4.14: a) Plots of $n(t)$ and $P(t)$ at the critical point for fractal dimension 1.5573. The hashed lines give the estimated values for the exponents outlined in Table 4.1. b) shows the plot of $R^2(t)$ with the hashed line showing the gradient $2/z$ with z given by the scaling relation (4.19). c) The double peaked histogram of population density indicating a first-order phase transition for $d_f \simeq 1.8928$. The inset shows the predicted values of $p_{d_c}(N)$ and an extrapolation of these results for $N \to \infty$. d) Possible power law behaviour for $d_f \simeq 1.7927$. The inset shows the lack of the double-peaked structure in the histogram.

Change from continuous to discontinuous transition at about $d_f = 1.7$

Conservation ecology

Size of refuge

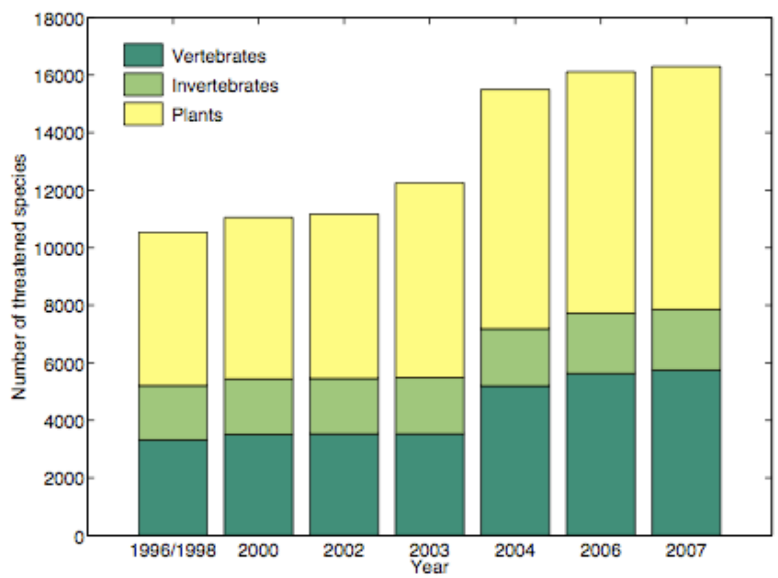

From
http://www.iucnredlist.org/info/2007RL Stats Table%202.pdf.

http://www.associatedcontent.com/image/16036/china_endangered_species_hunt.htm

Conservational implications of the model

- Analytic analysis of population dynamics equations like

$$\frac{\partial \rho(x,t)}{\partial t} = \mu\rho - \rho^2 + D\nabla^2\rho$$

conclude the existence of a threshold habitat size above which extinction won't occur.

- We find that size dependence is more subtle and strongly influenced by the existence of a critical point.
Fluctuations important.

A. Windus and H.J. Jensen
Allee Effects and Extinction in a Lattice Model.
Theo. Popul. Biol. 72, ,459-467 (2007).

Conservational implications of the model

- The need to find a mate introduces a direct density effect.

Increase p_d to 1 at t_k briefly to let population density drop to $\rho_\epsilon = \bar{\rho}_-$

Most run did result in extinction !

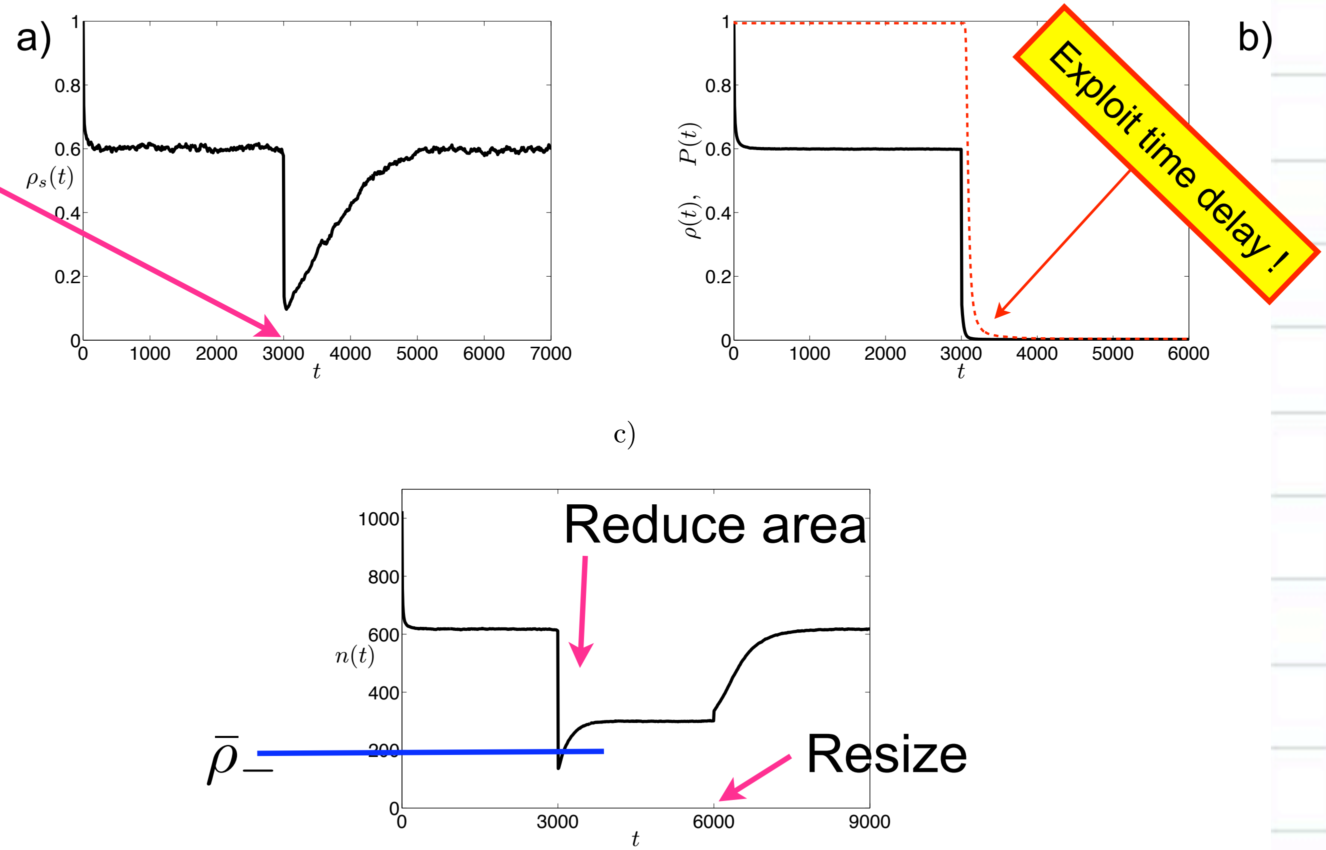

Figure 5.5: a) The average population density of the surviving runs only. b) The average population density of all the runs (solid line) and the survival probability $P(t)$ (hashed line), i.e. the probability that extinction has not occurred up to time t. c) Plot showing the recovery of the population density for the surviving runs only after a disease breakout at $t = 3000$ due to the re-sizing of the lattice. The lattice is returned to how it was originally at $t = 6000$ and the population recovers its original size.

Survival probability and habitat size

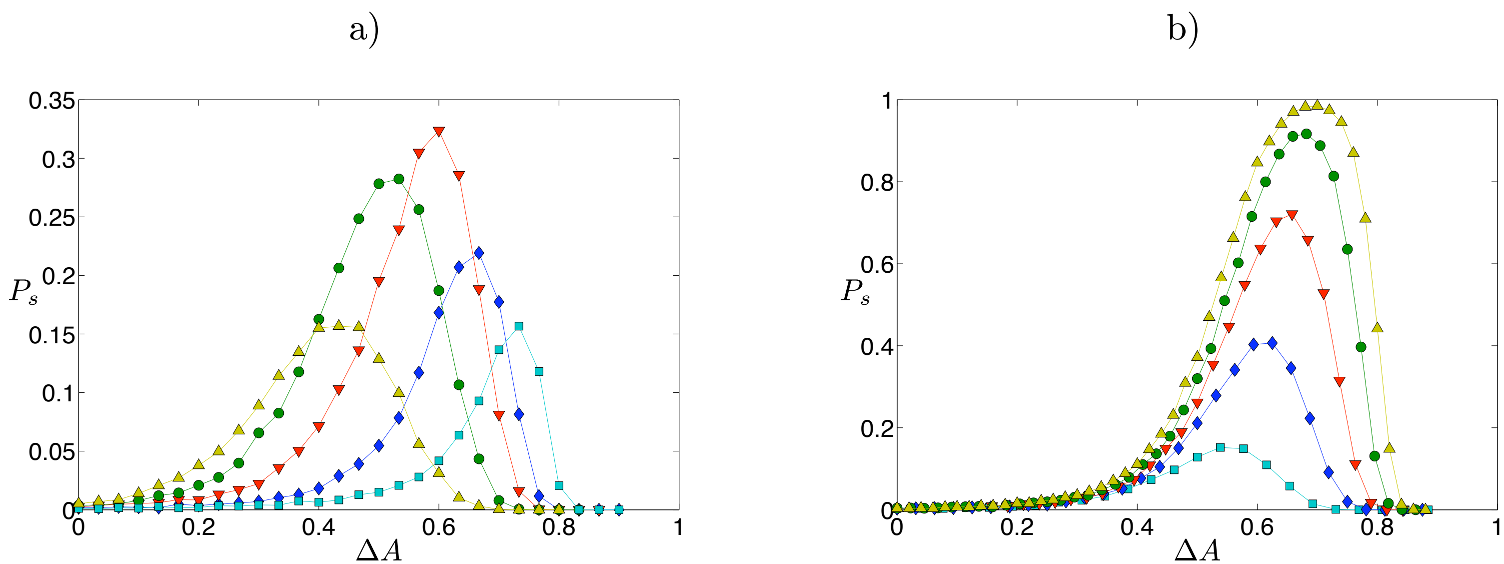

Figure 5.6: a) How the probability of survival changes with different reductions in habitat area, ΔA for $\rho_\epsilon = \rho_t = 0.05$ (□), 0.08 (◇), 0.11 (▽), 0.14 (○) and 0.17 (△). The corresponding values of p_d were 0.089, 0.091, 0.092, 0.093 and 0.094 respectively. b) How the probability of survival changes with reductions in habitat size, ΔA, for different initial values $L = 26$ (□), 32 (◇), 38 (▽), 44 (○) and 50 (△) with $\rho_\epsilon = \rho_t = 0.11$.

Mixture of asexual and sexual reproduction

All bacteria and viruses exhibit asexual reproduction. Fungi and Oomycetes can be asexual, sexual, or exhibit a mixture of both types of reproduction.

Darryl Stubbs

http://en.wikipedia.org/wiki/Oomycete

Tricritical behaviour

Generalised model.

asexual reproduction to occur with rate k

sexual reproduction as before occur with p_b

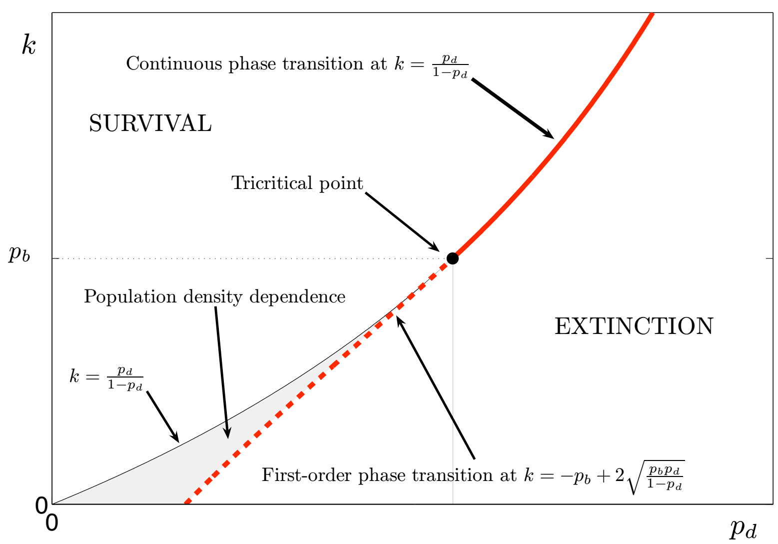

Figure 6.2: MF phase diagram showing the first-order and continuous phase transition lines. The tricritical point is also shown as well as the density-dependent region.

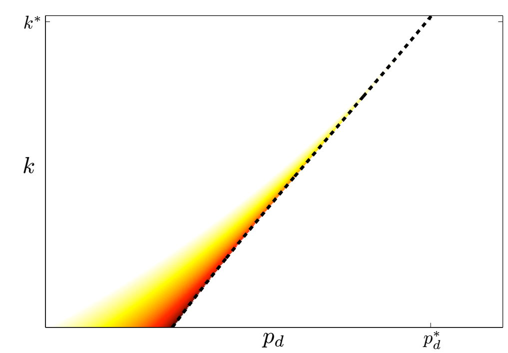

Figure 6.3: Plot showing how the value of the threshold population density varies across the density-dependent region. The darker the shade, the greater the value.

Relative rates of sexual asexual reproduction

Population structure at criticality.

For k=0.17 asexual rate = sexual rate

Concentrate on 2+1 dimensions

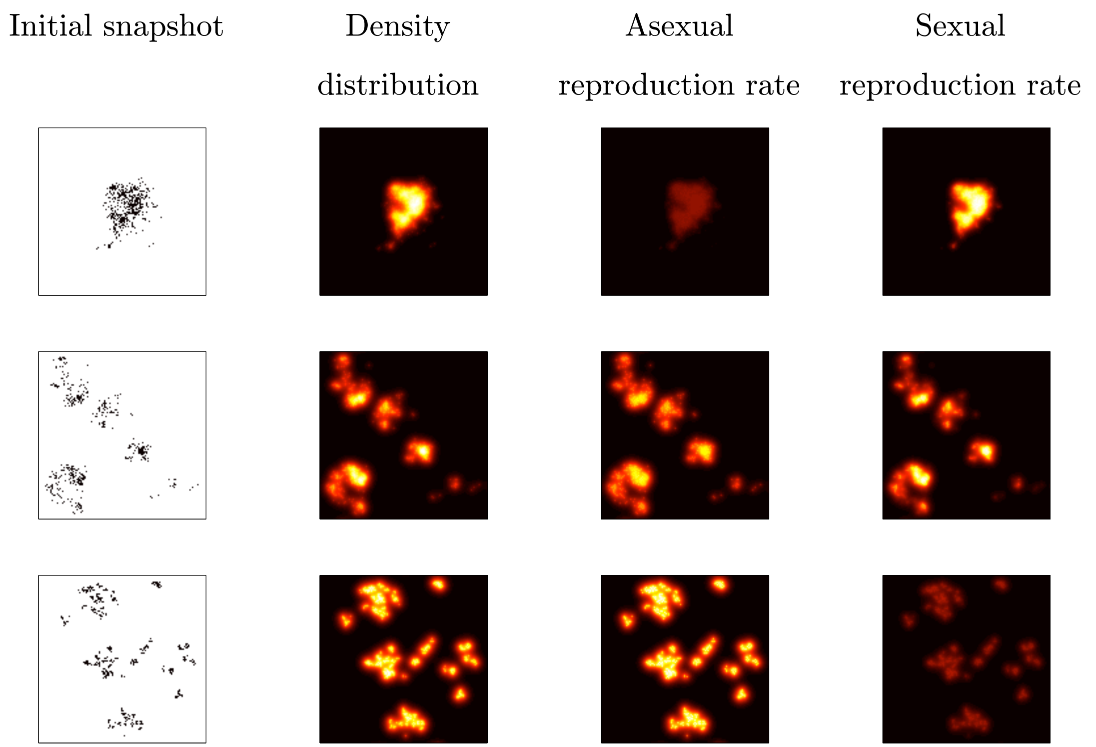

Figure 6.5: Plots of initial snapshots and average density distribution and relative reproduction rates over 50 time steps for (from top to bottom) $k = 0.05$, 0.17 and 1.0. The lighter colours indicates the greater probability for the latter three pictures in each row.

Sexual reproduction favoured in the denser areas

Tricritical: Monte Carlo & Mean field

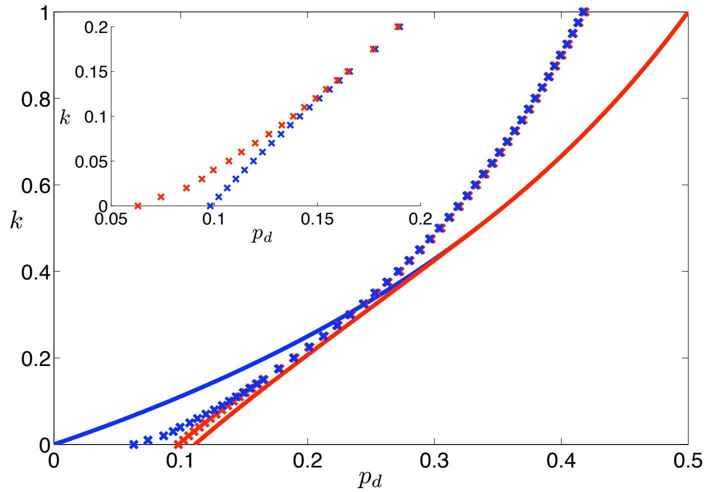

Figure 6.6: Phase diagram for the MF (lines) and simulation results (×). The red lines/markers show the critical points and the area in between the blue and red lines/markers shows the density-dependent region. The inset illustrates a zoomed-in region for the MC results only.

A. Windus and H.J. Jensen
Cluster geometry ans survival probability in systems driven by reaction diffusion dynamics
New J Phys 10, 113023 (2008)

Improved Mean Field

Cluster approximation

in one dimension

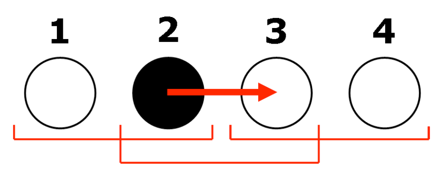

Henrik Jeldtoft Jensen

Imperial College London

Cluster approximation method

Reaction	$\Delta n_\bullet$	$\Delta n_{\bullet\bullet}$	Probability	
$\bullet\,\bullet\,\bullet \longrightarrow \bullet\,\circ\,\bullet$	-1	-2	$p_{\mathrm{d}}c^2/\rho$	
$\bullet\,\bullet\,\circ \longrightarrow \bullet\,\circ\,\circ$	-1	-1	$p_{\mathrm{d}}cd/\rho$	$\times 2$
$\circ\,\bullet\,\circ \longrightarrow \circ\,\circ\,\circ$	-1	0	$p_{\mathrm{d}}d^2/\rho$	
$\bullet\,\bullet\,\circ\circ \longrightarrow \bullet\,\circ\,\bullet\circ$	0	-1	$\frac{1}{2}(1-p_{\mathrm{d}})(1-k)cde/\rho(1-\rho)$	$\times 2$
$\circ\,\bullet\,\circ\bullet \longrightarrow \circ\,\circ\,\bullet\bullet$	0	$+1$	$\frac{1}{2}(1-p_{\mathrm{d}})(1-k)d^3/\rho(1-\rho)$	$\times 2$
$\bullet\,\circ\,\circ \longrightarrow \bullet\,\bullet\,\circ$	$+1$	$+1$	$\frac{1}{2}(1-p_{\mathrm{d}})kde/(1-\rho)$	$\times 2$
$\bullet\,\circ\,\bullet \longrightarrow \bullet\,\bullet\,\bullet$	$+1$	$+2$	$\frac{1}{2}(1-p_{\mathrm{d}})kd^2/(1-\rho)$	$\times 2$
$\bullet\,\bullet\,\circ\circ \longrightarrow \bullet\,\bullet\,\bullet\circ$	$+1$	$+1$	$\frac{1}{2}(1-p_{\mathrm{d}})p_{\mathrm{b}}cde/\rho(1-\rho)$	$\times 2$
$\bullet\,\bullet\,\circ\bullet \longrightarrow \bullet\,\bullet\,\bullet\bullet$	$+1$	$+2$	$\frac{1}{2}(1-p_{\mathrm{d}})p_{\mathrm{b}}cd^2/\rho(1-\rho)$	$\times 2$

Table 6.3: Reactions for the 2-site approximation. This time, reactions such as $\bullet\bullet\circ\bullet \longrightarrow \bullet\circ\bullet\bullet$ for which $\Delta n_\bullet = \Delta n_{\bullet\bullet} = 0$ have been ignored. A symmetry factor arising from the parity symmetry has also been included (right column) rather than writing both equations down.

A. Windus and H.J. Jensen
Accuracy of the cluster-approximation method in a nonequilibrium model.
J Stat Mech P03031 (2009)

Reaction			$\Delta n_{\bullet\bullet\bullet}$	$\Delta n_{\bullet\bullet\circ}$	$\Delta n_{\bullet\circ\circ}$	$\Delta n_{\bullet\circ\bullet}$	Probability	
○ ○ ● ○ ○	⟶	○ ○ ○ ○ ○	0	0	−1	0	$p_d z^2 w/d^2$	
○ ○ ● ○ ●	⟶	○ ○ ○ ○ ●	0	0	0	−1	$p_d zvw/d^2$	×2
○ ○ ● ● ○	⟶	○ ○ ○ ● ○	0	−1	0	0	$p_d y^2 z/cd$	×2
○ ○ ● ● ●	⟶	○ ○ ○ ● ●	−1	0	0	0	$p_d xyz/cd$	×2
○ ● ● ○ ●	⟶	○ ● ○ ○ ●	0	−1	1	−1	$p_d y^2 v/cd$	×2
○ ● ● ● ○	⟶	○ ● ○ ● ○	−1	−1	0	1	$p_d xy^2/c^2$	
○ ● ● ● ●	⟶	○ ● ○ ● ●	−2	0	0	1	$p_d x^2 y/c^2$	×2
● ○ ● ○ ●	⟶	● ○ ○ ○ ●	0	0	1	−2	$p_d v^2 w/d^2$	
● ○ ● ● ●	⟶	● ○ ○ ● ●	−1	0	1	−1	$p_d xyv/cd$	×2
● ● ● ● ●	⟶	● ● ○ ● ●	−3	1	0	1	$p_d x^3/c^2$	
○ ○ ● ○ ○●	⟶	○ ○ ○ ● ○●	0	0	−1	1	$\frac{1}{2}(1-p_d)(1-k)z^3 w/d^2 e$	×2
○ ○ ● ○ ●○	⟶	○ ○ ○ ● ●○	0	1	0	−1	$\frac{1}{2}(1-p_d)(1-k)zvw^2/d^3$	×2
○ ○ ● ○ ●●	⟶	○ ○ ○ ● ●●	1	0	0	−1	$\frac{1}{2}(1-p_d)(1-k)yzvw/d^3$	×2
○ ● ● ○ ○○	⟶	○ ● ○ ● ○○	0	−1	0	1	$\frac{1}{2}(1-p_d)(1-k)y^2 zu/cde$	×2
○ ● ● ○ ○●	⟶	○ ● ○ ● ○●	0	−1	−1	2	$\frac{1}{2}(1-p_d)(1-k)y^2 z^2/cde$	×2
○ ● ● ○ ●●	⟶	○ ● ○ ● ●●	1	−1	0	0	$\frac{1}{2}(1-p_d)(1-k)y^3 v/cd^2$	×2
● ○ ● ○ ○○	⟶	● ○ ○ ● ○○	0	0	1	−1	$\frac{1}{2}(1-p_d)(1-k)zuvw/d^2 e$	×2
● ○ ● ○ ●○	⟶	● ○ ○ ● ●○	0	1	1	−2	$\frac{1}{2}(1-p_d)(1-k)v^2 w^2/d^3$	×2
● ○ ● ○ ●●	⟶	● ○ ○ ● ●●	1	0	1	−2	$\frac{1}{2}(1-p_d)(1-k)yv^2 w/d^3$	×2
● ● ● ○ ○○	⟶	● ● ○ ● ○○	−1	0	0	1	$\frac{1}{2}(1-p_d)(1-k)xyzu/cde$	×2
● ● ● ○ ○●	⟶	● ● ○ ● ○●	−1	0	−1	2	$\frac{1}{2}(1-p_d)(1-k)xyz^2/cde$	×2
● ● ● ○ ●○	⟶	● ● ○ ● ●○	−1	1	0	0	$\frac{1}{2}(1-p_d)(1-k)xyvw/cd^2$	×2
○ ● ○ ○ ○	⟶	○ ● ● ○ ○	0	1	0	0	$\frac{1}{2}(1-p_d)kzuw/de$	×2
○ ● ○ ○ ●	⟶	○ ● ● ○ ●	0	1	−1	1	$\frac{1}{2}(1-p_d)kz^2 w/de$	×2
○ ● ○ ● ○	⟶	○ ● ● ● ○	1	1	0	−1	$\frac{1}{2}(1-p_d)kvw^2/d^2$	×2
○ ● ○ ● ●	⟶	○ ● ● ● ●	2	0	0	−1	$\frac{1}{2}(1-p_d)kyvw/d^2$	×2
● ● ○ ○ ○	⟶	● ● ● ○ ○	1	0	0	0	$\frac{1}{2}(1-p_d)kyzu/de$	×2
● ● ○ ○ ●	⟶	● ● ● ○ ●	1	0	−1	1	$\frac{1}{2}(1-p_d)kyz^2/de$	×2
● ● ○ ● ○	⟶	● ● ● ● ○	2	0	0	−1	$\frac{1}{2}(1-p_d)kyvw/d^2$	×2
● ● ○ ● ●	⟶	● ● ● ● ●	3	−1	0	−1	$\frac{1}{2}(1-p_d)ky^2 v/d^2$	×2
● ● ○ ○ ○	⟶	● ● ● ○ ○	1	0	0	0	$\frac{1}{2}(1-p_d)p_b yzu/de$	×2
● ● ○ ○ ●	⟶	● ● ● ○ ●	1	0	−1	1	$\frac{1}{2}(1-p_d)p_b yz^2/de$	×2
● ● ○ ● ○	⟶	● ● ● ● ○	2	0	0	−1	$\frac{1}{2}(1-p_d)p_b yvw/d^2$	×2
● ● ○ ● ●	⟶	● ● ● ● ●	3	−1	0	−1	$\frac{1}{2}(1-p_d)p_b y^2 v/d^2$	×2

Table 6.4: All reactions for the triplet approximation, where at least one of $\Delta n_{\bullet\bullet\bullet}$, $\Delta n_{\bullet\bullet\circ}$, $\Delta n_{\bullet\circ\circ}$ or $\Delta n_{\bullet\circ\bullet}$ is non-zero.

Behaviour for increasing n

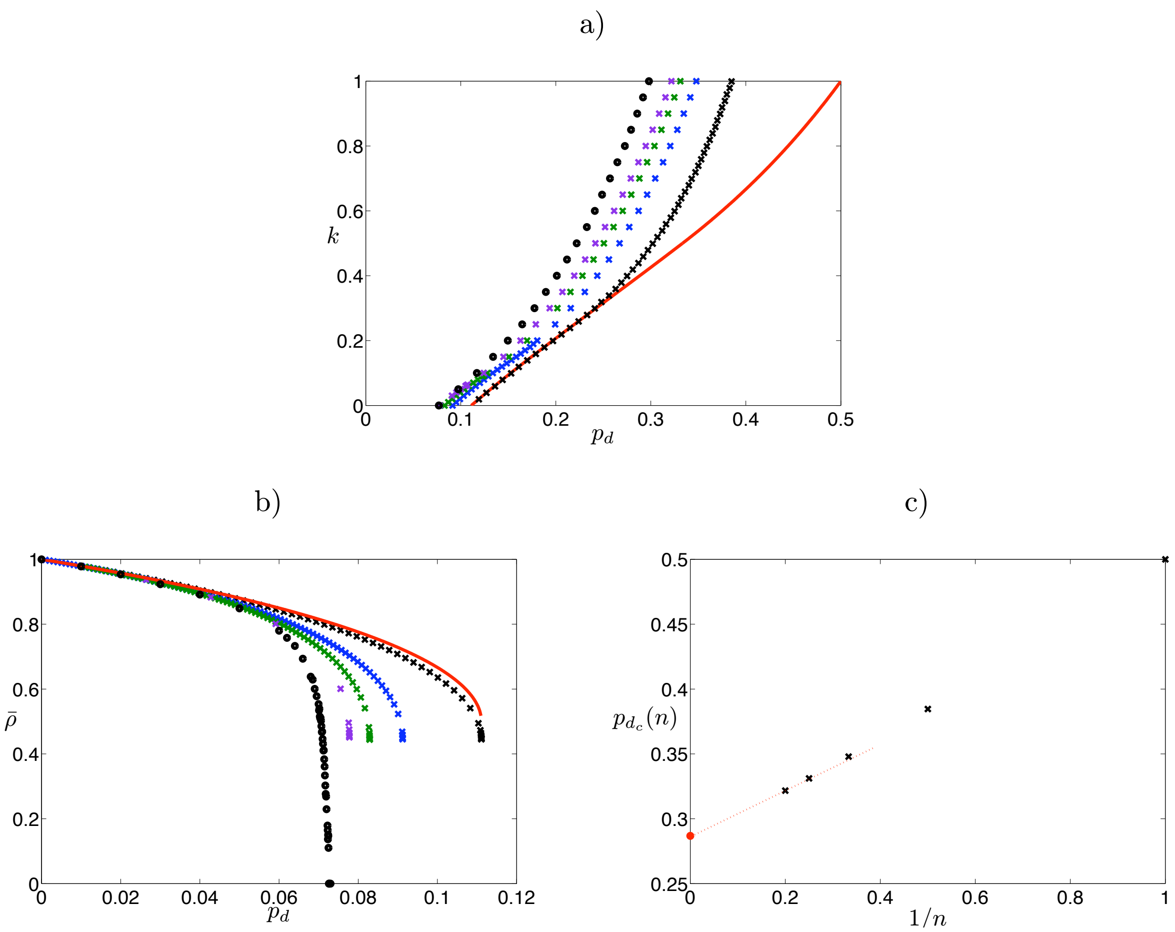

Figure 6.11: Numerical results for a) the critical point for various values of k and b) the steady state population density at $k = 0$. The red line shows the original MF approximation ($n = 1$) and the crosses (from right to left) the $n = 2$, 3, 4 and 5. The black circles illustrate the MC results. c) The approximation for p_{d_c} for $k = 1$ for the different values of n. The red circle shows the MC value with the red hashed line giving an extrapolation through the points for $n = 4$ and $n = 5$.

Behaviour for increasing n
Location of tricritical point - no good agreement

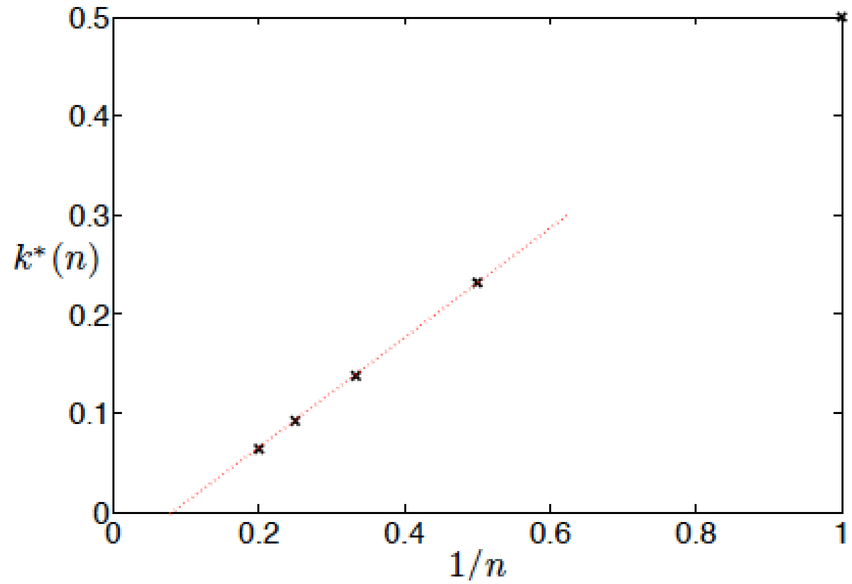

Figure 6.12: Plot showing how the approximated value of the tricritical point changes with n. The hashed red line is the straight line through the points from $n = 2$ to 5.

Geometrical structure of population

Simulations

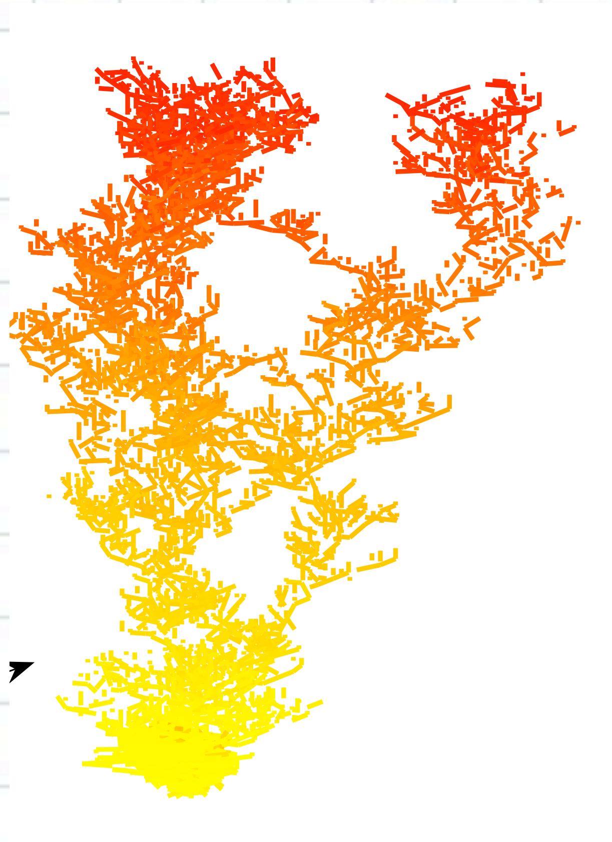

A. Windus and H.J. Jensen
Cluster geometry and extinction
in systems driven by reaction-diffusion dynamics.
New J of Physics 10, 113023 (2008)

Properties of individual clusters

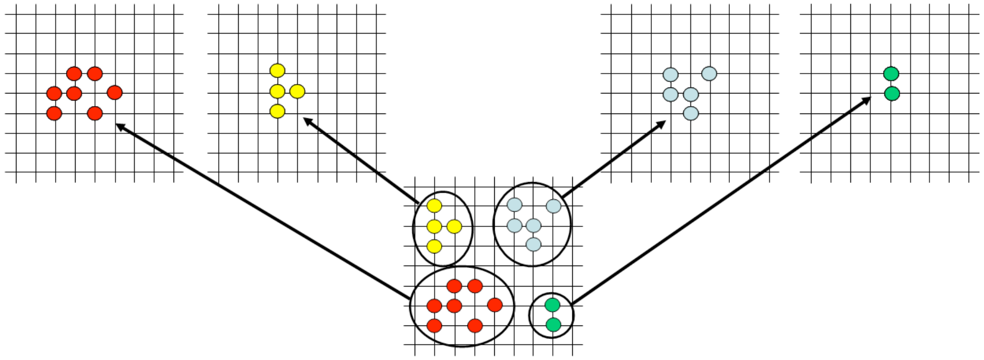

Figure 7.2: Picture of how the different clusters are taken from the original lattice and one by one are placed at the centre of a sufficiently large lattice.

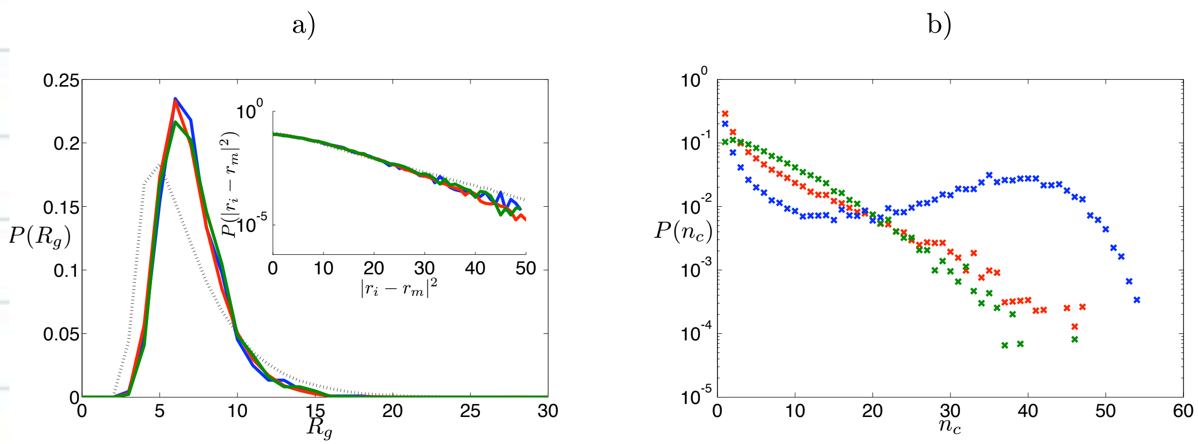

Figure 7.3: Histograms of a) R_g and $|\mathbf{r}_i - \mathbf{r}_\mathrm{m}|^2$ (inset) for clusters of size 20 and b) cluster size. In both plots we have $k = 0$ (blue), $k = 0.12$ (green) and $k = 1$ (red) and in a) only, the randomly formed clusters given by the hashed, black line.

Time-evolution of individual clusters

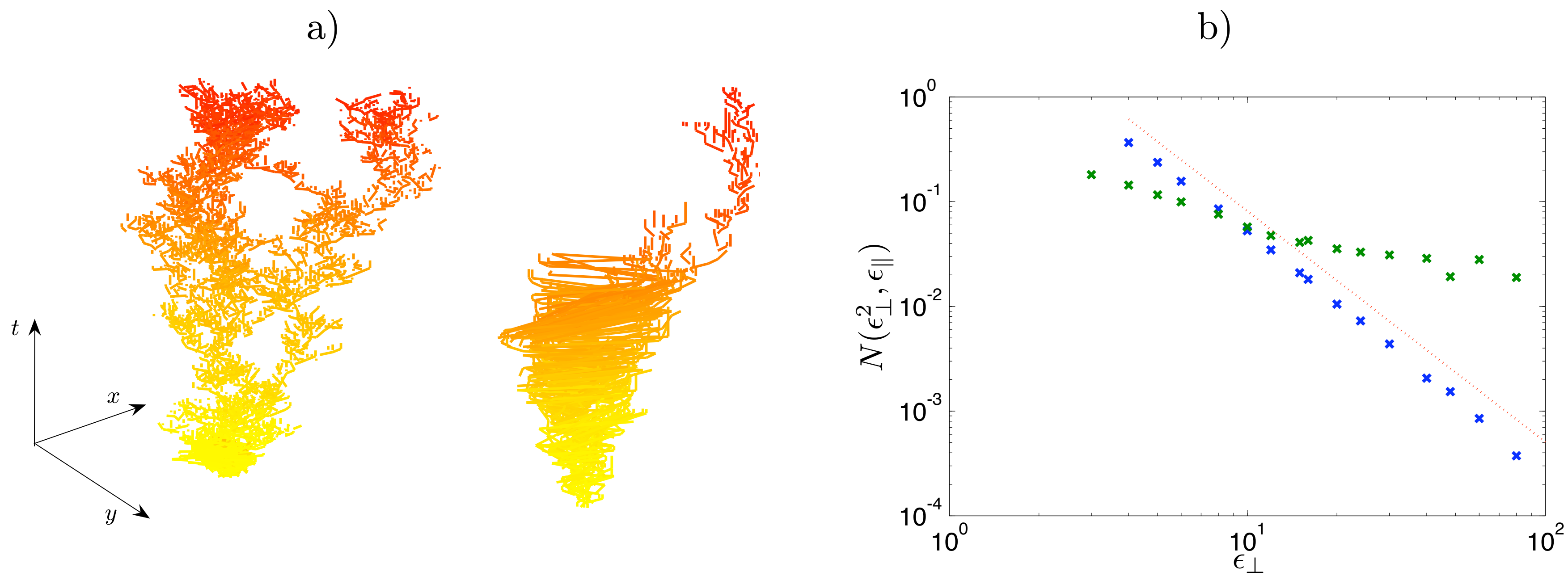

Figure 7.4: a) Space-time plots of a critical cluster beginning with two adjacent particles at the centre of an otherwise empty lattice for $k = 1$ (left) and $k = 0$ (right). b) The number of boxes $N(\epsilon_\perp^2, \epsilon_\parallel)$ of volume $\epsilon_\perp^2 \epsilon_\parallel$ needed to cover all of the occupied sites for $k = 1$ (blue) and $k = 0$ (green). The hashed line shows the DP value $D_f = 2.204$.

Cluster size and survival

Curve corresponding to the tricritical point: Linear dependence

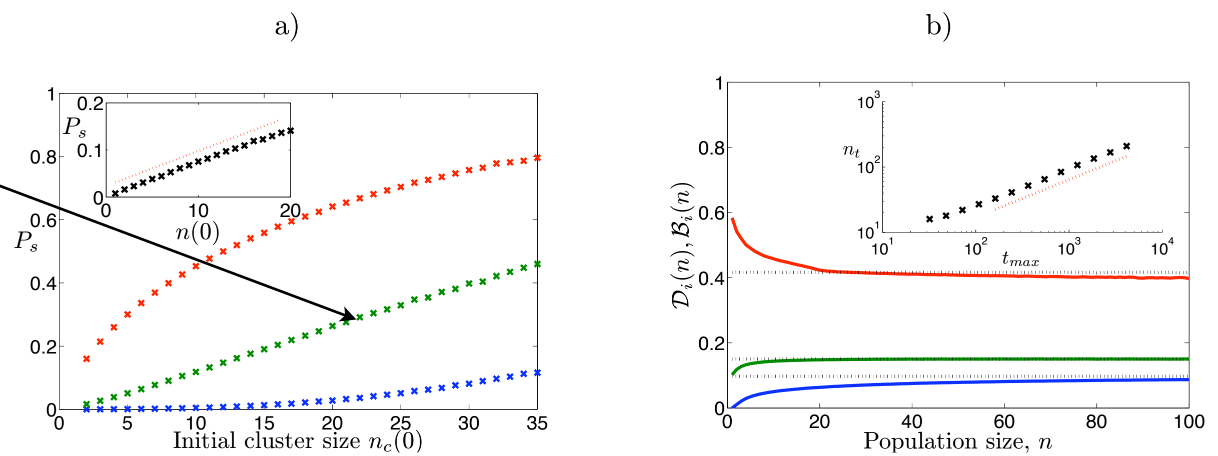

Figure 7.5: a) Plot of survival probability (for $t_{\max} = 200$) against initial cluster size for (from bottom to top) $k = 0$, 0.12 and 1. Relatively small cluster sizes were used since clearly $P_s \to 1$ as cluster size $\to \infty$. The inset shows P_s against population size, where the population increases with probability p and decreases by probability q as outlined in the text. The red hashed line shows true linear behaviour with gradient 0.0074. Equal values $p = q = 0.1502195$ were used with $t_{\max} = 1000$. b) The number of births (solid line) and deaths (hashed line) per individual per time step for (from bottom to top) $k = 0$, 0.12 and 1. The inset shows how, for $k = 1$, the position of the crossover for $\mathcal{B}_i(n)$ and $\mathcal{D}_i(n)$, n_c diverges to infinity with power law behaviour as $t_{\max} \to \infty$. The hashed line gives the gradient 0.576.

A. Windus and H.J. Jensen
Cluster geometry and extinction
Int J of Mod Phys C. **20**, 97 (2009)

Wednesday, 13 January 2010

Cluster size and survival

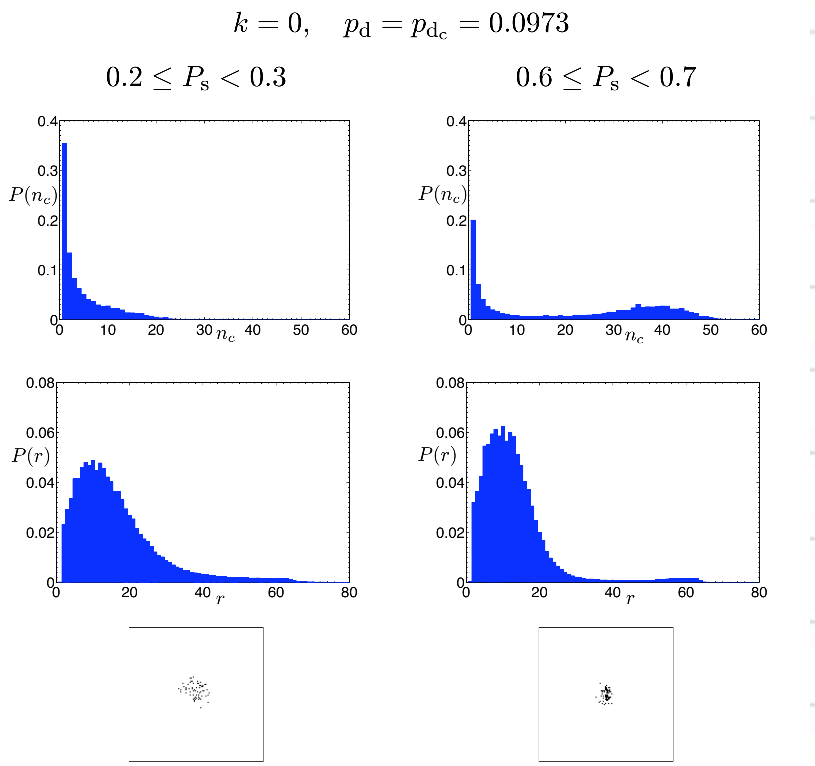

Purely asexual:
population consisting of
many small clusters best

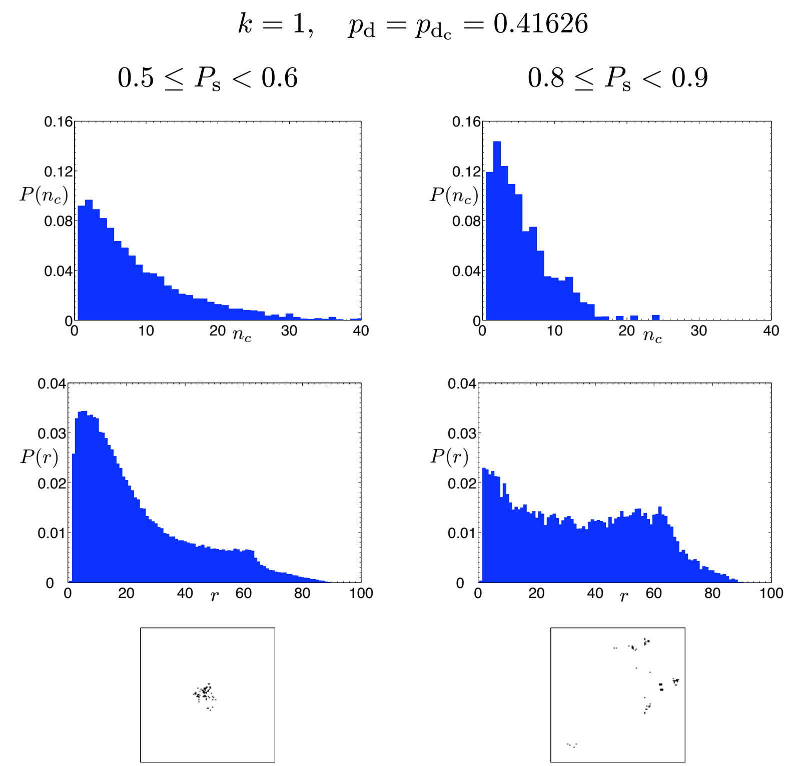

Purely sexual:
population consisting of
few large clusters best

Figure 7.9: For two values of k ($k = 0$ and $k = 1$), we plot (from top to bottom) histograms of cluster size n_c and distance between clusters r, and a typical snapshot of the population. For each value of k, we have combined all the population distributions whose survival probability P_s fell within the same range. We show both the highest and the lowest ranges of P_s for each value of k. A 128×128 lattice was used with $\rho_\epsilon = 64/128^2$.

Cluster size and survival

k=0.2

At k=0.2 no significant dependence on cluster distribution

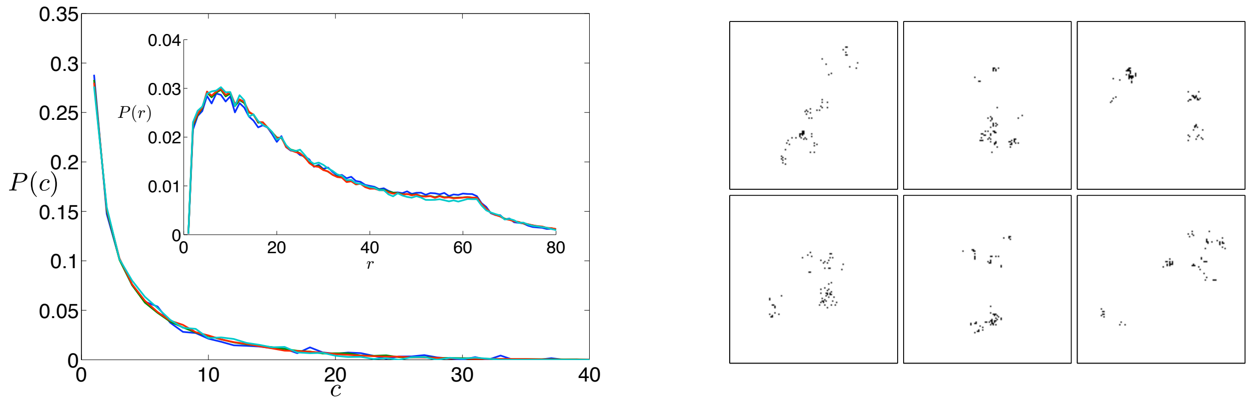

Figure 7.10: Histograms of cluster distribution for different ranges of P_s along with various snapshots of the population distributions for $k = 0.2$ and $p_d = p_{d_c} = 0.18888$. With $t_{max} = 500$, the top three snaphots had survival probabilities (from left to right) 0.42, 0.42 and 0.46 and the bottom three had probabilities 0.75, 0.75 and 0.76. We see no real difference between the cluster distributions for those that had a better chance of survival against those that had the worst, as verified by the collapsed histograms.

Situation different for k>0.2:
small well separated clusters best

Summary - conclusion

- Simple stat mech model - optimal refuge size + importance of fluctuations
- Focus on geometry of clusters

Thank you

References

A. Windus and H.J. Jensen, Phase transitions in a lattice population model.
J Phys A, 40, 2287-2297 (2007)

A. Windus and H.J. Jensen, Allee Effects and Extinction in a Lattice Model.
Theo. Popul. Biol. 72, 459-467 (2007)

A. Windus and H.J. Jensen, Cluster geometry and survival probability in systems driven by reaction diffusion dynamics
New J Phys 10, 113023 (2008)

A. Windus and H.J. Jensen, Accuracy of the cluster-approximation method in a nonequilibrium model
J Stat Mech P03031 (2009)

A. Windus and H.J. Jensen, Change in order of phase transition on fractal lattice.
Physica A **388**, 3107 (2009)

A. Windus and H.J. Jensen, Cluster geometry and extinction
Int J of Mod Phys C. **20**, 97 (2009)